Aggregated morphodynamic modelling of tidal inlets and estuaries

Wang, Zhengbing ; Townend, Ian; Stive, Marcel

DOI
10.1016/j.wse.2020.03.004

Publication date
2020

Document Version
Final published version

Published in
Water Science and Engineering

Water Science and Engineering 2020, 13(1): 1−13

HOSTED BY

ELSEVIER

Available online at www.sciencedirect.com

Water Science and Engineering

journal homepage: wse.hhu.edu.cn

Aggregated morphodynamic modelling of tidal inlets and estuaries

Zheng Bing Wang [a,b,c], Ian Townend [b,d,*], Marcel Stive [a,b]

[a] Faculty of Civil Engineering and Geosciences, Delft University of Technology, Delft 2600 GA, the Netherlands
[b] College of Harbor, Coastal and Offshore Engineering, Hohai University, Nanjing 210098, China
[c] Unit of Marine and Coastal Systems, Deltares, Delft 2600 MH, the Netherlands
[d] School of Ocean and Earth Sciences, University of Southampton, Southampton SO14 3ZH, UK

Received 16 September 2019; accepted 10 February 2020
Available online 26 March 2020

Abstract

Aggregation is used to represent the real world in a model at an appropriate level of abstraction. We used the convection-diffusion equation to examine the implications of aggregation progressing from a three-dimensional (3D) spatial description to a model representing a system as a single box that exchanges sediment with the adjacent environment. We highlight how all models depend on some forms of parametric closure, which need to be chosen to suit the scale of aggregation adopted in the model. All such models are therefore aggregated and make use of some empirical relationships to deal with sub-scale processes. One such appropriately aggregated model, the model for the aggregated scale morphological interaction between tidal basin and adjacent coast (ASMITA), is examined in more detail and used to illustrate the insight that this level of aggregation can bring to a problem by considering how tidal inlets and estuaries are impacted by sea level rise.

Keywords: Tidal inlet and estuary; Morphodynamic modelling; Aggregation; Temporal and spatial scales; Sea level rise; Sediment transport

1. Introduction

Morphodynamic modelling of coastal and estuarine systems has developed rapidly over the past 30 years, with many well-established modelling tools (e.g., Delft3D, FVCOM, and ASMITA), accompanied by guidance on the application of such models (e.g., Roelvink and Reniers, 2012, www.estuary-guide.net). Within this discipline, most research has focused on the development of numerical models that solve the flow and sediment transport equations to predict the change in morphology over estuary space scales and time scales from years to decades (e.g., Dam et al., 2016; van der Wegen et al., 2009). These models can be used to examine the evolution of tidal creeks, intertidal flats, and channels at the local scale, where the spatial resolution is on the order of tens of metres and the temporal resolution is seconds to hours. For morphological modelling, this is usually taken to be the micro-scale. Cowell et al. (2003) proposed a scale classification as follows: micro-scale (with a temporal scale from one second to one year and a spatial scale from 1 m to 1 km), meso-scale (with a temporal scale from one year to one thousand years and a spatial scale from 1 m up to 1 000 km), and macro-scale (with a temporal scale of millennia and a spatial scale greater than 1 000 km).

The models used at the micro-scale are typically governed by *fast* hydraulic flow simulations, which adopt some forms of the empirical relationship to deal with sub-scale processes, such as turbulence and bed friction. However, this is just one level of abstraction. Another well-established class of models is concerned with the meso-scale, where the focus is on the state of morphological features or the morphological system. This can be both qualitative for describing the state and system behaviour and quantitative for providing predictions at the feature/system scale. For the latter, the resolutions of space

* Corresponding author.
E-mail address: i.townend@soton.ac.uk (Ian Townend).
Peer review under responsibility of Hohai University.

https://doi.org/10.1016/j.wse.2020.03.004

and time are usually on the order of kilometres and decades to centuries, respectively.

The so-called regime theory is an example of analysis at the meso-scale. This has been extensively applied in rivers, estuaries, and deltas to describe key dimensions (e.g., width, depth, cross-sectional area, and ebb-tidal delta volume) based on the hydraulics and in particular the characteristic discharge of rivers or tidal channels (Lacey, 1930; Spearman, 2007). In the 1950s and 1960s, energy and entropy arguments were proposed as a theoretical basis to define the coefficients used in the earlier empirical hydraulic regime relationships, although this remains an area of some controversy (Langbein, 1963; Leopold and Langbein, 1962). Most recently, methods based on equilibrium sediment transport conditions have been used to define the system state (or regime) that is in equilibrium (Di Silvio, 1989; Stive and Wang, 2003). Although these models solve process equations that are similar to those used in micro-scale models, as described above, the integration is over larger (meso) spatial and temporal scales, and they have been variously referred to as aggregated, box, and semi-empirical models in the literature. However, the classification of those models as semi-empirical is misleading because all models across all scales use some forms of parametric closure based on empirical relations to solve the governing equations. The closure of the governing equations is generally at an appropriate level of the process formulation, e.g., for small-scale models, the closure is at the level of the friction and/or the turbulence; for meso-scale models, the closure is at the level of the aggregated sediment transport; and for large-scale models, the closure is at the level of the morphological elements, e.g., the entire ebb-tidal delta of a tidal inlet.

For morphological modelling, the meso-scale class of models has proved particularly useful when examining a long-term change related to engineering and coastal management problems. However, there remains a lack of clarity about how this type of models relates to models used at the micro-scale. To address this, we provide a detailed account of the progressive stages of aggregation used to move from a three-dimensional (3D) spatial description to an aggregated box model description. We then use the resulting mathematical description to illustrate the insights that aggregation at the macro-scale can offer. Whilst these insights could probably have also been developed at the micro-scale, this would require huge numbers of simulations and would still lack the clarity offered by the relatively simple expressions developed through an aggregation at an appropriate scale, i.e., the scale of interest.

2. Stages of aggregation (from micro- to meso-scales)

In order to clarify the link between micro-scale and meso-scale models, we made use of the convection-diffusion equation, as used in many coastal and estuarine morphological models, to examine the implications of aggregation progressing from a 3D spatial description (which itself involves aggregation in the closure terms) to a model representing a system as a single box that exchanges sediment with the outside environment. The aggregation steps are described below.

2.1. 3D to 2D aggregation at micro-scale

We start with the 3D convection-diffusion equation governing the sediment concentration:

$$\frac{\partial c}{\partial t}+\frac{\partial (u_x c)}{\partial x}+\frac{\partial \left(u_y c\right)}{\partial y}+\frac{\partial (u_z c)}{\partial z}-\frac{\partial}{\partial x}\left(\varepsilon_x \frac{\partial c}{\partial x}\right)-\frac{\partial}{\partial y}\left(\varepsilon_y \frac{\partial c}{\partial y}\right)= w_s \frac{\partial c}{\partial z}+\frac{\partial}{\partial z}\left(\varepsilon_z \frac{\partial c}{\partial z}\right) \tag{1}$$

where c is the sediment concentration; t is time; u_x, u_y, and u_z are the flow velocity components in the x-, y-, and z-directions, respectively; ε_x, ε_y, and ε_z are the turbulent diffusion coefficients in the x-, y-, and z-directions, respectively; and w_s is the settling velocity. This is in fact the mass conservation equation for sediment transport, forming the kinetic part of the theory for suspended sediment transport. The dynamic part of the theory for suspended sediment transport is reflected by the bed boundary condition. At the boundary near the bed, the sediment concentration, or the sediment concentration gradient, can be prescribed. Their values can be calculated using a sediment transport formula (in the case of sand) or a formulation for the erosion rate (in the case of mud).

Eq. (1) can be integrated in the vertical direction to obtain the depth-averaged advection-diffusion equation:

$$\frac{\partial (h\overline{c})}{\partial t}+\frac{\partial (\alpha_x \overline{u}_x h\overline{c})}{\partial x}+\frac{\partial \left(\alpha_y \overline{u}_y h\overline{c}\right)}{\partial y}-\frac{\partial}{\partial x}\left(D_x h\frac{\partial \overline{c}}{\partial x}\right)- \frac{\partial}{\partial y}\left(D_y h\frac{\partial \overline{c}}{\partial y}\right)=f_b \tag{2}$$

where the over-bar represents depth-averaging of the corresponding variable; h is the water depth; α_x and α_y are the coefficients accounting for the effects of the flow velocity and sediment concentration distributions in the x- and y-directions, respectively; D_x and D_y are the dispersion coefficients in the x- and y-directions, respectively; and f_b is the sediment exchange flux between the bed and the water column.

This can be considered the first level of aggregation used by many micro-scale models. Note that the diffusion coefficients in the horizontal direction become dispersion coefficients as they also represent the mixing due to the non-uniform vertical distributions of flow velocity and sediment concentration.

2.2. 2D to 1D aggregation at micro-scale

The next level of aggregation can be carried out by integrating Eq. (2) over the width of a river, estuary, or channel:

$$\frac{\partial (A\overline{c})}{\partial t}+\frac{\partial (\alpha \overline{u}_x A\overline{c})}{\partial x}-\frac{\partial}{\partial x}\left(AD_x\frac{\partial \overline{c}}{\partial x}\right)=F_b \tag{3}$$

where the over-bar represents averaging over the cross-section, A is the cross-sectional area, α is the coefficient accounting for

the effects of the distributions of flow velocity and sediment concentration within the cross-section, and F_b is obtained through integration of f_b over the width. This is the equation for suspended sediment concentration used in 1D network models.

Eq. (3) can also be written as

$$\frac{\partial(h\bar{c})}{\partial t}+\frac{\partial s_x}{\partial x}+\frac{\partial s_y}{\partial y}=f_b \tag{4}$$

where s_x and s_y are the suspended sediment transport rates in the x- and y-directions, respectively. This equation can be further aggregated by integrating over a part of or the whole estuary (a morphological element). Using Green's theorem, the integration yields

$$\frac{\partial(VC)}{\partial t}=\sum_i J_i+F_B \tag{5}$$

where V is the volume of the water body of the area, J_i is the sediment transport at the open boundary i (a positive sign means that the transport is directed to an element, i.e., import), F_B is obtained through integration of f_b over a morphological element, and C is the average sediment concentration in the element. This equation can also be derived by considering the mass balance of sediment in the whole water body.

2.3. Further aggregation in space and time at meso-scale

Eqs. (2)−(5) can also be aggregated in time, e.g., over a tidal period or a much longer time. As an example, integration of Eq. (3) over a tidal period yields

$$\frac{\partial(u_{xr}h\bar{c})}{\partial x}+\frac{\partial\left(u_{yr}h\bar{c}\right)}{\partial y}-\frac{\partial}{\partial x}\left(D_x h\frac{\partial\bar{c}}{\partial x}\right)-\frac{\partial}{\partial y}\left(D_y h\frac{\partial\bar{c}}{\partial y}\right)=f_b \tag{6}$$

The first term in Eq. (2), representing the change of sediment storage in the water column, is neglected as it becomes much less important at longer time scales than the term on the right-hand side representing the sediment exchange with the bed. All the other terms remain basically the same, but the parameters and variables now represent the tidally averaged values. The residual flow velocities (u_{xr} and u_{yr}) cause advection, and the tidal flow now becomes the major mixing agent for the dispersion represented by the coefficients D_x and D_y, as elaborated by Wang et al. (2008).

Aggregation of Eq. (5) in time yields the following equation used in an aggregated model for the aggregated scale morphological interaction between tidal basin and adjacent coast (ASMITA, Stive and Wang, 2003):

$$\sum_i J_i+F_B=0 \tag{7}$$

2.4. Sediment exchange between bed and water column

The advection-diffusion equation describes a mass balance for suspended sediment transport, no matter what level of aggregation is adopted. It does not describe any dynamics but only the kinetics of suspended sediment transport, because the equation itself does not provide the information about the flux of sediment exchange between the bed and the water column. In its aggregated forms (Eqs. (2)−(7)), this flux is expressed with a term in the equation. It cannot be determined by solving the equation, but needs to be prescribed. In fact, this flux determines the morphological change as well, and its formulation represents the dynamic part of the suspended sediment transport model.

For the 3D form (Eq. (1)), the dynamic part is introduced via the bed boundary condition. At the boundary near the bed, the sediment concentration, the vertical gradient of the sediment concentration, or a linear combination of the two factors can be prescribed. When prescribing the sediment concentration, it is often argued that the concentration near the bed can instantaneously adjust to the local flow condition, and therefore the equilibrium value of sediment concentration can be prescribed. In fact, for steady uniform flow, the solution for the vertical profile of sediment concentration, far away from the boundary, is the equilibrium concentration profile. The prescribed value of sediment concentration at the bed boundary is therefore by definition the equilibrium concentration. A similar argument can be made for the prescribed concentration gradient at the bed. Physically, by prescribing the sediment concentration, the vertical sediment flux due to settling is given but the vertical flux due to turbulent mixing is left undefined. However, by prescribing the concentration gradient, the opposite is true. For non-cohesive sediment, the required equilibrium concentration or the equilibrium concentration gradient depends on the flow conditions and the sediment properties and can be determined with one of the many sediment transport formulas (e.g., Soulsby, 1997; van Rijn, 1993). Note that the equilibrium values of sediment concentration and its gradient are related to each other as the downwards flux due to settling and the upwards flux due to turbulent mixing balance each other out at equilibrium. For cohesive sediment, deposition and erosion rates according to the Krone-Partheniades formulation are often used for the bed boundary condition. According to this formulation, deposition occurs only when bed shear stress τ is below a critical value τ_d, and erosion occurs only when bed shear stress is above another critical value τ_e. With this formulation it is always impossible to define the instantaneous equilibrium concentration by balancing the deposition and erosion rates. For $\tau_d<\tau_e$, this leads to an equilibrium concentration equal to zero for $\tau<\tau_d$, an equilibrium concentration undetermined for $\tau_d<\tau<\tau_e$, and an equilibrium concentration infinitely large for $\tau>\tau_e$. However, if the hydrodynamic condition is fluctuating due to some factors, e.g., tides, a tide-averaged equilibrium concentration can be defined. Recently, Winterwerp et al. (2012) argued that deposition always takes place, i.e., τ_d should be infinitely large. With this approach it is then possible to define the instantaneous equilibrium concentration for mud.

The advection-diffusion equations when aggregated in space but not in time (Eqs. (2) and (3)) are also used in micro-scale models. The flux f_b or F_b can be calculated with the

Krone-Partheniades formulation for cohesive sediment, or with a formulation derived from an asymptotic solution of the 3D advection-diffusion equation (Galappatti and Vreugdenhil, 1985; Wang, 1992) for non-cohesive sediment. These formulations require information concerning hydrodynamic conditions expressed with the flow velocity $\overline{u}$, bed shear stress τ, etc., in addition to the sediment properties, e.g., the median grain size of sediment D_{50}:

$$f_b = F(\overline{u}, \tau, D_{50}, \cdots) \tag{8}$$

When the advection-diffusion equations are aggregated in time, the detailed information on hydrodynamic conditions required by a sediment transport formula or the Krone-Partheniades formulation is no longer available. The sediment exchange flux between the bed and the water column needs to be expressed with available aggregated morphological and hydrodynamic parameters. This formulation, representing the dynamics of sediment, is dependent on the level of aggregation, which is a key difference from other models. The formulations often have the following form:

$$f_b = \gamma w_s (c_e - c) \tag{9}$$

where γ is a dimensionless coefficient, and c_e is the equilibrium sediment concentration. This is similar to the formulation of Galappatti and Vreugdenhil (1985) for micro-scale models. The difference between the models is the way in which c_e is calculated.

Di Silvio (1989) related the equilibrium concentration to the morphological state variable. As an example, for shoals influenced by wind waves, he used

$$c_e \propto h^{-n} \tag{10}$$

where n is a power. It is noted that this relation implicitly defines the morphological equilibrium, at which c_e is equal to the sediment concentration prescribed at the open boundary of the model.

In the ESTMORF model (Wang et al., 1998) and the ASMITA model (Stive et al., 1998), the equilibrium concentration is dependent on the ratio between the morphological state variables and its equilibrium value. As an example, for the channels in the ESTMORF model, the formulation is

$$c_e = c_E \left(\frac{A_e}{A} \right)^n \tag{11}$$

where A_e is the equilibrium value of the cross-sectional area, and c_E is the global equilibrium concentration. When the whole system is in morphological equilibrium, $c = c_e = c_E$. The rationale behind this formulation is that the ratio A_e/A is an indication of the flow strength in the channel with respect to equilibrium, as A_e increases with the increasing tidal prism. The formulation is thus analogous to a power law for sediment transport capacity.

3. Modelling at meso-scale

Describing the system in terms of larger-scale morphological elements has the advantage that empirical relations are available for morphological equilibrium. In contrast, the detailed micro-scale models often encounter difficulties in correctly reproducing, or even achieving, morphological equilibrium. However, the aggregation in the meso-scale schematisation also introduces difficulties in the description/representation of the hydrodynamics in sediment transport processes. To avoid such difficulties, the classic aggregated morphodynamic models assume exponential decays of disturbances with respect to morphological equilibrium (Eysink, 1990). The decay time scales are often empirically derived. Therefore, these models have been called empirical models. To our knowledge, Di Silvio (1989) and Di Silvio et al. (2010) were the first to introduce a suspended sediment transport module into an aggregated (in time) morphodynamic model. The long-term averaged sediment concentration field is simulated directly with an advection-diffusion equation, just like a micro-scale model that solves the instantaneous sediment concentration field. In addition, the local equilibrium value for the long-term averaged suspended sediment concentration is defined and related to the local morphological state variable following some physical arguments, and again this is conceptually the same as a micro-scale model. As an example, the equilibrium value of the long-term averaged sediment concentration on shoals is argued to be inversely proportional to a power of the local water depth for given wind and wave climates. By relating the local equilibrium sediment concentration to the morphological equilibrium, the aggregated morphodynamic models for ESTMORF (Wang et al., 1998) and ASMITA (Spearman, 2007; Stive et al., 1998; Stive and Wang, 2003; Townend et al., 2016a) have been developed. These models have proved to be effective for modelling long-term morphological development in estuaries (Townend et al., 2007; Wang and Townend, 2012) and tidal inlet systems (Kragtwijk et al., 2004; van Goor et al., 2003). They combine the empirical relations for morphological equilibrium with process modelling of suspended sediment transport and therefore have often been classified as hybrid or semi-empirical models.

The previous section makes it clear that the essential difference between meso-scale and micro-scale models (e.g., ASMITA and Delft3D) is the level of aggregation rather than the degree in which their formulations contain empirical elements. They both use the advection-diffusion equation for modelling the suspended sediment transport. The formulations concerning sediment dynamics, i.e., the exchange between the bed and the water column, contain empirical elements in both models. The ASMITA model makes use of the empirical relations for morphological equilibrium and Delft3D uses a sediment transport formula, which is also empirical in character. The empirical elements in both models also involve the

same degree of uncertainty. In this sense, it is not meaningful to classify the two types of models as respectively (semi-) empirical and process-based. These models only differ in the level of abstraction that is used to represent the real world.

In addition to the aggregation level and the formulation for the sediment exchange flux between the bed and the water column, the hydrodynamic module helps to differentiate various models. Obviously, the implemented hydrodynamic module depends to a large extent on the aggregation level of the model. As an example, the models for ESTMORF (Wang et al., 1998) and ASMITA (Stive et al., 1998) are based on the same type of formulations. However, the ESTMORF model can be coupled to a (micro-scale) 1D network hydrodynamic model to simulate the required aggregated hydrodynamic parameters, e.g., the tidal volume and tidal range, as various other hybrid models (e.g., O'Connor et al., 1990; Wright and Townend, 2006). In contrast, due to a higher level of spatial aggregation, the ASMITA model calculates the tidal prism for the prescribed tidal range and plan area. Micro-scale models can be 1D, 2D, or 3D, depending on the hydrodynamic module.

The ASMITA formation was first proposed by Stive et al. (1998) for modelling long-term morphological development of tidal inlet systems in the Dutch Wadden Sea. A tidal inlet system is schematised into a limited number of morphological elements, at a level like an ebb-tidal delta, as described by Walton and Adams (1976). For each element, a water volume below a certain reference level or a sediment volume above a certain reference plane (not necessarily horizontal) acts as the integral state variable. A tidal inlet system is typically schematised into the following three elements (Fig. 1): an ebb-tidal delta, with the total excess sediment volume relative to an undisturbed coastal bed profile (V_d) determined as its state variable; an intertidal flat area in the tidal basin, with the total sediment volume between the mean low water (MLW) and mean high water (MHW) (V_f) determined as its state variable; and a channel area in the tidal basin, with the total water volume below MLW (V_c) determined as its state variable. The hydrodynamic and morphological parameters are defined according to Lodder et al. (2019).

Fig. 1 shows that the adjacent coastal areas, which can exchange sediment with the inlet system, are considered an open boundary. Tidal flats are depicted with a sediment volume (Fig. 1(c)), but it is also possible to represent tidal flats with the volume of water over the tidal flats (Townend et al., 2016a).

Although commonly used for a tidal inlet system, this three-element schematisation is not the only possible schematisation. In fact, an ASMITA model can contain any number of inter-connected morphological elements. It is relevant to mention that the ASMITA model was applied to the Dutch Wadden Sea basins based on the assumption that the flood-tidal delta extends over the whole back-barrier basin, although it is not generally the case. The US east coast has many tidal basins, with a flood-tidal delta confined to a location near the inlet opening. This would require a different set of elements to represent the system.

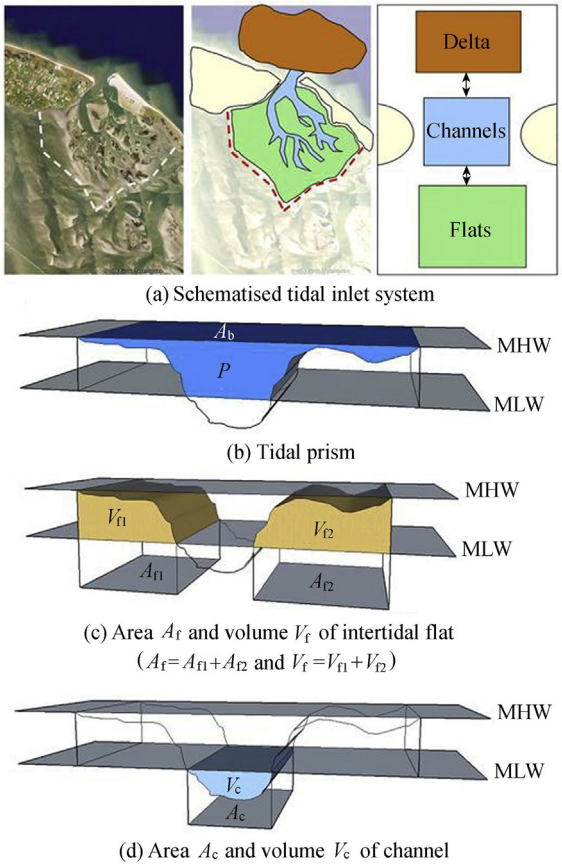

Fig. 1. Three-element schematisation for a tidal inlet system in ASMITA model.

Anyhow, a necessary requirement is that the morphological equilibrium of each element is defined and can be evaluated with the available (aggregated) hydrodynamic parameters in the model. In the following section, this three-element schematisation is used to explain the model formulation and to demonstrate some applications. In addition, a one-element model is used to explain certain points, in which a whole back-barrier basin of the tidal inlet system is considered a single morphological element with the water volume below MHW in the basin as the state variable.

The formulation of the ASMITA model has been detailed in various publications (Stive et al., 1998; van Goor et al., 2003; Kragtwijk et al., 2004; Townend et al., 2016a, 2016b). For completeness, the basis of a three-element model suitable for the exploration of the impacts of sea level rise on tidal inlets and estuaries is provided in Appendix.

4. Impact of sea level rise on tidal inlets

Aggregation to a particular scale allows the modeller to focus on system states, or flows in and out of the system. Choosing an appropriate scale of aggregation can make certain problems more tractable, or provide greater insight into the system dependencies. This is illustrated by considering the sensitivity of tidal inlets to sea level rise, using the formulation derived for the meso-scale. For simplicity's sake, we adopted

the ASMITA formulation for a single element (combined channel and tidal flat with no delta). Previous work examined the potential for tidal inlet systems to drown (Rossington et al., 2007; van Goor et al., 2003). The analysis that follows is similar but has more detail, to highlight how the various system parameters influence the sensitivity of the system to sea level rise.

The one-element ASMITA model for a tidal basin with the water volume below MHW, V, as the state variable, is as follows:

$$\frac{\mathrm{d}V}{\mathrm{d}t}=\frac{w\delta c_{\mathrm{E}}A_{\mathrm{b}}}{\delta+wA_{\mathrm{b}}}\left[\left(\frac{V_{\mathrm{e}}}{V}\right)^{n}-1\right]+A_{\mathrm{b}}R \tag{12}$$

where V_{e} is the equilibrium volume (without sea level rise) of the tidal basin, R is the sea level rise rate, A_{b} is the horizontal area of the basin at MHW, w is the vertical sediment exchange velocity, and δ is the horizontal sediment exchange coefficient. The details about exchange and transport of sediment are explained in Appendix. A dynamic equilibrium is achieved for a constant rate of sea level rise if the volume V is constant, with $\mathrm{d}V/\mathrm{d}t = 0$.

The dynamic equilibrium is possible only if R is smaller than a critical value R_{c}, with

$$R_{\mathrm{c}}=\frac{w\delta c_{\mathrm{E}}}{\delta+wA_{\mathrm{b}}} \tag{13}$$

For the dynamic equilibrium state, we have

$$\frac{V}{V_{\mathrm{e}}}=\left(1-\frac{R}{R_{\mathrm{c}}}\right)^{-\frac{1}{n}} \tag{14}$$

This solution is depicted in Fig. 2 for $n = 2$. A linear model is derived by linearizing Eq. (12) around $V = V_{\mathrm{e}}$, which is also shown in Fig. 2:

$$\frac{\mathrm{d}V}{\mathrm{d}t}=\frac{V_{\mathrm{e}}-V}{T}+A_{\mathrm{b}}R \tag{15}$$

where T is the morphological time scale, and

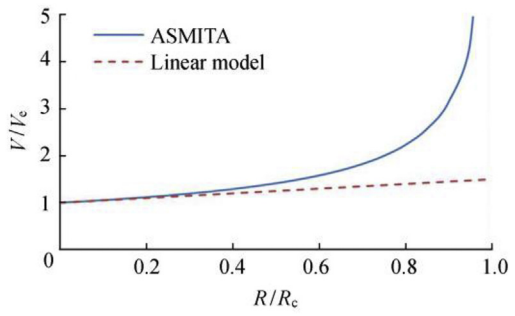

Fig. 2. V/V_{e} vs. R/R_{c}.

$$T=\frac{1}{nc_{\mathrm{E}}}\left(\frac{V_{\mathrm{e}}}{wA_{\mathrm{b}}}+\frac{V_{\mathrm{e}}}{\delta}\right) \tag{16}$$

Comparison of Eqs. (13) and (16) yields a relation between T and R_{c} as follows:

$$R_{\mathrm{c}}=\frac{V_{\mathrm{e}}}{nTA_{\mathrm{b}}} \tag{17}$$

A dynamic equilibrium for a constant rate of sea level rise is again achieved if V no longer changes with time, with $\mathrm{d}V/\mathrm{d}t = 0$. This leads to

$$V=V_{\mathrm{e}}+A_{\mathrm{b}}RT=V_{\mathrm{e}}\left(1+\frac{R}{nR_{\mathrm{c}}}\right) \tag{18}$$

4.1. Assessing sensitivity of system to rate of sea level rise

Considering the system as a single element, a non-linear equation can be used to determine the sensitivity of the system to a given (constant) rate of sea level rise, as indicated by Eq. (13). The limiting rate of sea level rise is determined by four parameters, and it is instructive to examine how the limiting rate of sea level rise varies with these parameters. Typical ranges for each parameter are defined in Table 1. The way in which each of these parameters influences the limiting rate of sea level rise is shown in Fig. 3.

The joint influence of the parameters is illustrated in Fig. 4. Fig. 4(a) shows the joint influence of the size of the basin and the availability of sediment. Fig. 4(b) shows the joint influence of the horizontal sediment exchange coefficient and vertical sediment exchange velocity.

4.1.1. Relative importance of parameters

For the range of parameters considered, there is a similar degree of sensitivity of the basin size, the vertical sediment exchange velocity, and the horizontal sediment exchange coefficient to the limiting rate of sea level rise (Fig. 3(a)−(c)). There is a much larger variation of the limiting rate of sea level rise for the range of equilibrium sediment concentration considered (Fig. 3(d)). This range represents the state from a limited sediment supply to a relatively turbid system and highlights the importance of sediment supply. The basin size can have a significant effect on the system's ability to keep pace with the sea level rise. Large basins with a limited sediment supply are more likely to drown and small basins with a plentiful sediment supply should be able to maintain their form even if the rate of sea level rise increases

Table 1
Typical ranges for parameters that determine limiting rate of sea level rise for single element.

Parameter	Range	Parameter	Range
w	1×10^{-5}−1×10^{-3} m/s	c_{E}	2×10^{-5}−2×10^{-4}
δ	500−3 000 m^3/s	A_{b}	1−100 km^2

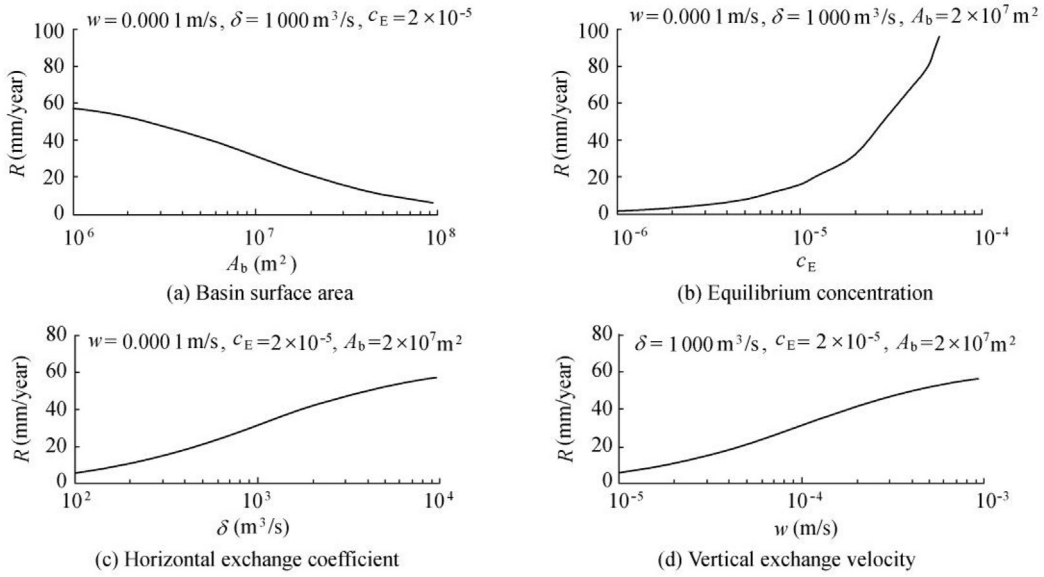

Fig. 3. Plots to illustrate limiting rate of sea level rise varying with different parameters.

dramatically. In a similar manner, an increasing sediment supply increases the resilience of the system to a rapid sea level rise. Moreover, a large horizontal exchange coefficient and a high velocity of vertical sediment exchange with the bed may both reduce the vulnerability of the system to a rapid sea level rise.

4.1.2. Sensitivity of system to sea level rise

Fjords, fjards, and rias all have limited sediment supply. Arguably, fjords and fjards are drowned systems. However, the potential consequence for rias, as found in the southwest of the UK, is that they can also be progressively drowned as a result of high rates of sea level rise. For coastal plain, tidal inlets, and drowned valley systems, the system setting is important. Systems under macro-tidal conditions are likely to be less vulnerable than those under micro-tidal conditions because of the higher horizontal sediment exchange rate. Similarly, sandy systems are likely to be less sensitive than muddy ones because the vertical sediment exchange rate is higher (sand has a larger settling velocity). However, in all cases, the availability of sediment is critical. The background supply may be suspended load or bed load and may be sourced from the river or the marine environment. In this model this is represented by the equilibrium sediment concentration, an important parameter for assessing whether the system remains healthy or degrades, as illustrated by the changes in Venice over the last two centuries (Townend, 2010).

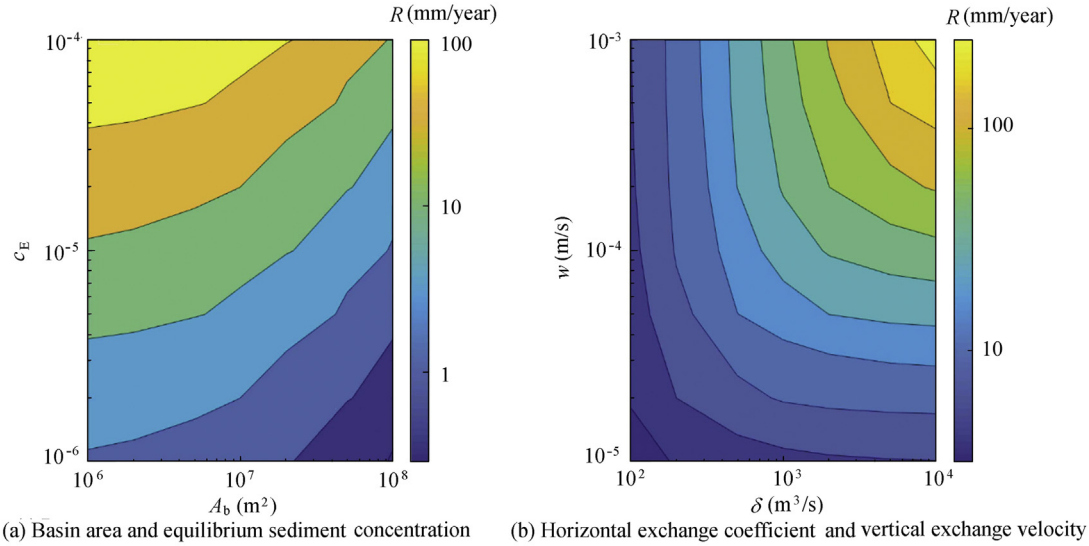

Fig. 4. Limiting rate of sea level rise under joint influence of parameters.

It is important to recognize that Eq. (12) treats the estuarine system as a single element. This is, of course, a gross simplification. The ASMITA model subdivides the system into the main geomorphological elements, namely channel, tidal flat, and delta. Introducing this additional subdivision results in different responses for the different types of elements. In most cases, the tidal flats (comprising a smaller volume and being furthest from the source of sediment) are significantly more sensitive to the sea level rise than the tidal channel and delta components of the estuary. Consequently, several studies have shown that estuarine systems including tidal flats have the capacity to adapt to rates of sea level rise in the range of 5−30 mm/year (Rossington et al., 2007).

4.2. Application of ASMITA model

The ASMITA model is meant for simulating long-term large-scale morphological development of tidal inlet systems. It was originally developed for the tidal inlet systems in the Dutch Wadden Sea (Stive et al., 1998). The first applications to the Dutch Wadden Sea concerning the responses of the tidal inlet systems to human interferences (Kragtwijk et al., 2004) and to sea level rise (van Goor et al., 2003) were summarized by Stive and Wang (2003). Later, the model was applied to the Dutch Wadden Sea in environmental impact assessment studies for gas and salt mining and to other systems in the world, including estuaries (Townend et al., 2007; Rossington et al., 2007). It has also been implemented as a module in the DIVA model for evaluating the impact of climate change on the worldwide coastal system (Hinkel et al., 2013). More discussion on the ASMITA model and its applications can be found in Townend et al. (2016a, 2016b). Here we discuss an application of the model to evaluating the impact of relative sea level rise on the Dutch Wadden Sea tidal inlet systems.

The Dutch Wadden Sea consists of a series of tidal inlets with their tidal basins (Fig. 5). Multiple large- and small-scale

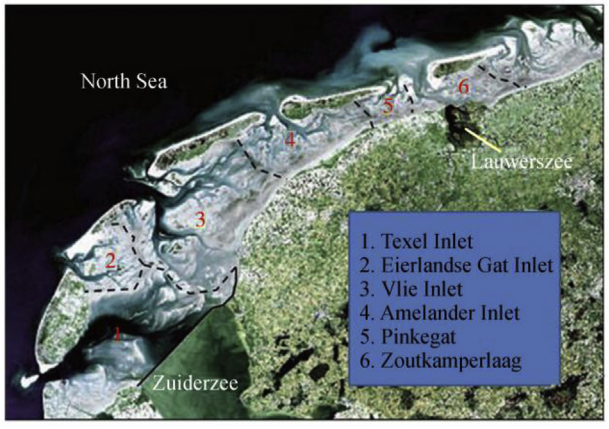

Fig. 5. Tidal basins in Dutch Wadden Sea.

human interventions in the past have basically fixed the boundaries of the Dutch Wadden Sea. The two recent major interventions were the closures of the Zuiderzee in 1932 and the Lauwerszee in 1969, and they are still influencing the morphological development (Elias et al., 2012; Wang et al., 2012, 2018). Due to the closure of the Zuiderzee, the western part of the Dutch Wadden Sea (Texel, Eierlandse Gat, and Vlie inlets) is still far from morphodynamic equilibrium (Wang et al., 2018).

Historically, the morphological development of this system, consisting of barrier islands separated by tidal inlets and back-barrier basins with channels, tidal flats, and saltmarshes, has been closely related to the sea level rise. It was formed about 7 000 years ago under the influence of a rising sea level. The development of basins depends on the balance between sediment accretion and the relative sea level rise rate (Nichols, 1989). Beyond a critical rate of relative sea level rise at approximately 1 m per century, sediment import becomes insufficient, resulting in drowning of the basins (Carrasco et al., 2016; Deltacommissie, 2008; Stive et al., 1990; van der Spek and Beets, 1992; van Goor et al., 2003). The relative sea level rise is the sea level rise plus the sea floor subsidence due to, e.g., gas and salt mining.

Anticipating that worldwide sea level rise will accelerate (KNMI, 2017; Le Bars et al., 2017; Meehl et al., 2007), studies on the Dutch Wadden Sea have been carried out, resulting in a series of position papers coordinated by the Wadden Academy in the Netherlands. Vermeersen et al. (2018) projected three scenarios for future sea level rise in the Dutch Wadden Sea until 2100, following the representative concentration pathways (RCP2.6, RCP4.5, and RCP8.5). Fokker et al. (2018) predicted sea floor subsidence due to gas and salt mining in the coming decades. The morphological response of the Dutch Wadden Sea to the sea level rise and sea floor subsidence (together the relative sea level rise) was projected by Wang et al. (2018), on the basis of the ASMITA model results and supported by observations concerning the morphological development since 1926. The ASMITA model used was the same as the approach of van Goor et al. (2003), with the most up-to-date parameter settings of the ASMITA model for the tidal inlet systems of the Dutch Wadden Sea shown in Tables 2−4.

Following the approach of van Goor et al. (2003), the results are presented as the probability of drowning as a function of the rate of sea level rise, which has been obtained by considering all the relevant model parameters as stochastic variables. Based on this probability distribution, an uncertainty range for the critical rate of sea level rise can be obtained, as shown in Table 5. In this table, the value of the rate of sea level rise corresponding to a probability of 16% for drowning is the median value minus the standard deviation (if the distribution is a normal one). However, the values for the Texel and Vlie inlets appear to be unrealistic, as the lower limits are lower than the observed sedimentation rates in the past. The

Table 2
Tidal ranges and morphological parameters of three elements.

Inlet	H (m)	A_f (km^2)	A_c (km^2)	A_d (km^2)	V_{f0} (10^6 m^3)	V_{c0} (10^6 m^3)	V_{d0} (10^6 m^3)
Texel	1.65	133.0	522.0	92.53	51.5	2 160.0	509.1
Eierlandse Gat	1.65	105.0	52.7	37.80	55.0	106.0	132.0
Vlie	1.90	328.0	387.0	106.00	162.0	1 230.0	369.7
Amelander	2.15	178.0	98.3	74.70	120.0	302.0	131.0
Pinkegat	2.15	38.1	11.5	34.00	29.6	18.5	35.0
Zoutkamperlaag	2.25	65.0	40.0	78.00	69.0	177.0	151.0

Note: H is the tidal range; A_f, A_c, and A_d are the horizontal areas of the tidal flat, channel, and ebb-tidal delta, respectively; and V_{f0}, V_{c0}, and V_{d0} are the initial values of V_f, V_c, and V_d in 1970, respectively.

Table 3
Parameters influencing morphological time scale.

Inlet	n	c_E	w_f (m/s)	w_c (m/s)	w_d (m/s)	δ_{od} (m^3/s)	δ_{dc} (m^3/s)	δ_{cf} (m^3/s)
Texel	2	0.000 2	0.000 1	0.000 10	0.000 01	1 550	2 450	980
Eierlandse Gat	2	0.000 2	0.000 1	0.000 05	0.000 01	1 500	1 500	1 000
Vlie	2	0.000 2	0.000 1	0.000 10	0.000 01	1 770	2 560	1 300
Amelander	2	0.000 2	0.000 1	0.000 05	0.000 01	1 500	1 500	1 000
Pinkegat	2	0.000 2	0.000 1	0.000 10	0.000 01	1 060	1 290	840
Zoutkamperlaag	2	0.000 2	0.000 1	0.000 10	0.000 01	1 060	1 290	840

Note: w_f, w_c, and w_d are the vertical sediment exchange velocities of the tidal flat, channel, and ebb-tidal delta, respectively; and δ_{od}, δ_{dc}, and δ_{cf} are the horizontal sediment exchange coefficients from the outside area to the ebb-tidal delta, from the ebb-tidal delta to the channel, and from the channel to the tidal flat, respectively.

observed sedimentation rates at these two inlets are about the same as the sea level rise rate corresponding to the probability of 30% for drowning. Therefore, the range based on the probability of 30% is also given in Table 5. The median values of the critical sea level rise rate, corresponding to a probability of 50%, are used for the projections of the morphological response.

Table 4
Parameters for defining morphological equilibrium.

Inlet	V_{fe} (10^6 m^3)	a_c (10^{-6})	a_d (10^{-3})
Texel	151.00	10.000	4.025
Eierlandse Gat	57.83	13.130	8.000
Vlie	190.00	9.600	2.662
Amelander	131.20	10.241	2.921
Pinkegat	30.30	10.140	6.927
Zoutkamperlaag	70.00	27.266	9.137

Note: V_{fe} is the equilibrium value of V_f, and a_c and a_d are the coefficients accounting for the effects of the distributions of flow velocity and sediment concentration within the cross-section of the channel and ebb-tidal delta, respectively.

Table 5
Critical sea level rise rates for tidal basins in Dutch Wadden Sea for five values of probabilities of drowning.

Probability (%)	Critical sea level rise rates for different tidal basins (mm/year)					
	Texel	Eierlandse Gat	Vlie	Amelander	Pinkegat	Zoutkamperlaag
16	4.5	11.6	4.1	6.7	21.1	11.1
30	5.5	14.2	5.0	8.2	25.8	13.5
50	7.0	18.0	6.3	10.4	32.7	17.1
70	8.1	20.9	7.3	12.1	37.9	19.8
84	9.5	24.4	8.5	14.1	44.3	23.1

By comparing the median values in this table to the sea level rise scenarios presented by Vermeersen et al. (2018) and the sea floor subsidence projections by Fokker et al. (2018), Wang et al. (2018) concluded that the critical rate of relative sea level rise will not be exceeded for the RCP2.6 scenario in any of the basins in the Dutch Wadden Sea. For the RCP4.5 scenario, it will be exceeded only in the Vlie Inlet Basin starting from 2030; for the RCP8.5 scenario, it will be exceeded in the Texel Inlet Basin starting from 2050, in the Vlie Inlet Basin from 2030, and in the Amelander Inlet Basin from 2100. It is noted that exceedance of the critical value does not mean that a tidal basin will drown (loss of all intertidal flats) immediately. In fact, it is concluded that none of the considered tidal basins will drown before 2100, even for the RCP8.5 scenario. However, the accelerated sea level rise will cause loss of part of the intertidal flats. The loss will be noticeable in 2050 for the RCP8.5 scenario and in 2100 for the RCP4.5 scenario.

5. Conclusions

Aggregation is a valuable means by which a modeller can focus on representing the real world at an appropriate level of abstraction, choosing the attributes and system states of interest. A very crude abstraction may provide simplicity but insufficient resolution of the problem, whereas inclusion of too much detail may make the model computationally intensive, or even intractable. Hence the correct choice is important for efficiency but more important for the clarity of insight that can be obtained.

Using morphological models of tidal inlets and estuaries as an example, we have shown that the aggregation is a process of progressively grouping terms, or integrating over spatial and temporal scales. Thus, in the example presented, the models at the different scales (micro and meso) solve the same equations just at different levels of resolution. Importantly, some forms of empirical closure scheme are needed at all scales. Hence, the models are all empirical to some degree.

The insights to be obtained from aggregation to the scale of interest have been illustrated for the case of sea level rise. With some manipulation of the governing equations at the meso-scale it is possible to show how a tidal inlet subject to sea level rise is likely to respond, as a function of system size, tidal range, sediment supply, and type of sediment. Such a relatively simple examination of the key dimensions of the problem would be much harder to achieve using an equivalent micro-scale model.

Acknowledgements

This study was carried out within the framework of the Coastal Genesis 2 Project funded by Rijkswaterstaat, and co-funded by Netherlands Organization for Scientific Research (NWO) via the SEAWAD Project and the Dutch Royal Academy of Sciences via the project of Coping with Deltas in Transition within the framework of Programme Scientific Strategic Alliances between China and the Netherlands.

Appendix: Aggregated morphodynamic modelling of tidal inlets and estuaries

The bases of the hydrodynamics, morphological equilibrium state, sediment transport, and morphological changes used in the ASMITA model are detailed below. This tidal inlet sytem is presented in terms of three geomorphological elements, namely delta, channel, and tidal flat. The details of the formulation of an ASMITA model using multiple elements can be found in Kragtwijk et al. (2004) and Townend et al. (2016a, 2016b).

A.1. Hydrodynamics

If the morphology of a tidal inlet system is only defined by the volumes of the three morphological elements mentioned above (see Fig. 1), it does not need to model the hydrodynamics in detail. In fact, only the tidal range in the back-barrier basin and the tidal prism are needed to define the morphological equilibrium state. Tidal basins, such as those in the Dutch Wadden Sea, are relatively small with respect to the tidal wavelength. For such small basins it is acceptable to use the water volume between the mean low water (MLW) and mean high water (MHW) for the tidal prism. When the intertidal volume is defined in terms of sediment volume, the relation between the tidal range H and the tidal prism P is as follows:

$$P = A_b H - V_f \tag{A.1}$$

where A_b is the horizontal area of the basin at MHW, and V_f is the total sediment volume between MLW and MHW. The tidal range in the basin is dependent on the tidal range in the open sea and the morphological state of the tidal inlet system. The tidal range in the open sea should be considered a boundary condition. It is difficult to model the influence of the morphological changes on the tidal range due to the highly aggregated schematisation. However, for small basins like those in the Dutch Wadden Sea, the influence of the morphological changes on the tidal range is limited. Therefore, the tidal range in the basin H is prescribed. It is noted that it is still possible to have H varying with time, to take account of any trend or a cyclic change, e.g., the nodal tide variation (Jeuken et al., 2003; Wang and Townend, 2012). It is also noted that the model does consider the feedback from the morphological development to the hydrodynamics, via Eq. (A.1), because V_f is a morphological state variable.

A.2. Morphological equilibrium state

For all three elements, empirical relationships are required to define their morphological equilibrium dimensions. With these relationships the morphological equilibrium state of a tidal basin is fully determined if the basin area A_b and the tidal range H are given. The equilibrium relationships can be prescribed in various ways (see Townend et al., 2016a, 2016b). Here we outline the approach that has been used to study the dynamics of the Dutch Wadden Sea.

For the intertidal flat there are two empirical relationships used, one for its area and the other for its height (Renger and Partenscky, 1974; Eysink and Biegel, 1992):

$$\frac{A_{fe}}{A_b} = 1 - 2.5 \times 10^{-5} \sqrt{A_b} \tag{A.2}$$

$$h_{fe} = \alpha_{fe} H \tag{A.3}$$

where A_{fe} is the equilibrium tidal flat surface area in m^2, and h_{fe} is the equilibrium height of the tidal flat. According to Eysink (1990), $\alpha_{fe} = \alpha_f - 0.24 \times 10^{-9} A_b$, with $\alpha_f = 0.41$.

The equilibrium volume of the intertidal flat, i.e., the equilibrium sediment volume between MLW and MHW, is given as

$$V_{fe} = A_{fe} h_{fe} \tag{A.4}$$

The channel volume V_c is defined as the water volume under MLW in the tidal basin. Its equilibrium value is related to the tidal prism as follows:

$$V_{ce} = \alpha_c P^{1.55} \tag{A.5}$$

where α_c is an empirical coefficient.

The equilibrium volume of the ebb-tidal delta is also related to the tidal prism (Walton and Adams, 1976) as follows:

$$V_{de} = \alpha_d P^{1.23} \tag{A.6}$$

where α_d is an empirical coefficient.

Using these equations with various empirical coefficients α_c and α_d, the morphological equilibrium of a tidal basin can be determined with two parameters, the total basin area A_b and the tidal range H, with $V_e = F(A_b, H)$, where V_e is the equilibrium volume of the basin. For a one-element model for the back-barrier basin, the total water volume of the basin below MHW, V, which is the sum of the channel volume (below LHW) V_c and the tidal prism P, can be expressed as $V = V_c + P$.

A.3. Sediment transport and morphological change

As explained in the previous section, the sediment transport processes are described by the mass balance equation for sediment for each element aggregated in time (Eq. (7)). Following the schematisation shown in Fig. 1, these equations are

$$J_{cf} + F_{Bf} = 0 \tag{A.7}$$

$$J_{dc} - J_{cf} + F_{Bc} = 0 \tag{A.8}$$

$$J_{od} - J_{dc} + F_{Bd} = 0 \tag{A.9}$$

where J is the sediment transport, with the subscripts indicating the transport directions, in which the subscripts f, c, d, and o mean the intertidal flat, channel, ebb-tidal delta, and outside area, respectively. J_{cf} is thus the sediment transport from the channel to the intertidal flat. F_{Bf}, F_{Bc}, and F_{Bd} are sediment exchange flux between the bed and the water column of the intertidal flat, channel, and ebb-tidal delta, respectively. Because of the aggregation in time, the transports are governed by the diffusion/dispersion with the tidal flow as mixing agent:

$$J_{cf} = \delta_{cf}(c_c - c_f) \tag{A.10}$$

$$J_{dc} = \delta_{dc}(c_d - c_c) \tag{A.11}$$

$$J_{od} = \delta_{od}(c_o - c_d) \tag{A.12}$$

where c is the suspended sediment concentration, and its subscript indicates the morphological element. δ is the horizontal exchange coefficient, which depends on the dispersion coefficient, the area of the cross-section connecting the two elements, and the distance between the two elements (see Wang et al., 2008). Its subscripts have similar meanings as those of J.

F_B is the sediment exchange flux between the bed and water column, representing the erosion minus sedimentation. F_{Bf}, F_{Bc}, and F_{Bd} are formulated as follows:

$$F_{Bf} = w_f A_f (c_{fe} - c_f) \tag{A.13}$$

$$F_{Bc} = w_c A_c (c_{ce} - c_c) \tag{A.14}$$

$$F_{Bd} = w_d A_d (c_{de} - c_d) \tag{A.15}$$

where A_f, A_c, and A_d are the horizontal areas of the intertidal flat, channel, and ebb-tidal delta, respectively; c_{fe}, c_{ce}, and c_{de} are the equilibrium sediment concentrations of the intertidal flat, channel, and ebb-tidal delta, respectively; and w_f, w_c, and w_d are the vertical sediment exchange velocities of the intertidal flat, channel, and ebb-tidal delta, respectively, which are proportional to the settling velocity of sediment. Note that the vertical exchange velocity is not necessarily the same for all three elements even if only a single fraction of sediment is present. As discussed earlier, the equilibrium sediment concentrations for the elements are calculated by comparing the morphological state with its equilibrium state:

$$c_{fe} = C_f \left(\frac{V_f}{V_{fe}}\right)^{n_f} \tag{A.16}$$

$$c_{ce} = C_c \left(\frac{V_{ce}}{V_c}\right)^{n_c} \tag{A.17}$$

$$c_{de} = C_d \left(\frac{V_d}{V_{de}}\right)^{n_d} \tag{A.18}$$

where C_f, C_c, and C_d are coefficients for different elements, with the dimension of sediment concentration; and n is a power similar to that in a power-law sediment transport formula (Wang et al., 2008), with the subscripts indicating the morphological elements. Note that there is a difference in the formulations between the elements of the intertidal flat and ebb-tidal delta with a sediment volume as a morphological state variable and the channel element with a water volume as a state variable (sediment volume relationships are the inverse of the water volume relationships).

The sediment exchange between the bed and water column (Eqs. (A.13)−(A.15)) also determines the change of the morphological state variable of the corresponding element, with $dV_f/dt = -F_{Bf}$, $dV_c/dt = F_{Bc}$, and $dV_d/dt = -F_{Bd}$. If all the morphological elements in the whole system are in equilibrium, F_B should vanish for all elements. Thus, the sediment concentration is equal to its equilibrium value for each of the elements, with $c_f = c_{fe}$, $c_c = c_{ce}$, and $c_d = c_{de}$. Eqs. (A.7)−(A.9) yield $J_{cf} = J_{dc} = J_{od} = 0$, i.e., all residual sediment transports vanish, followed by $c_f = c_c = c_d = c_o$ from Eqs. (A.10)−(A.12), and also $c_{fe} = c_{ce} = c_{de}$. According to Eqs. (A.16)−(A.18), $c_{fe} = C_f$, $c_{ce} = C_c$, and $c_{de} = C_d$ if all the elements are in equilibrium (their volumes are equal to their equilibrium values), and then, $C_f = C_c = C_d = c_o$. Thus, the coefficients in Eqs. (A.16)−(A.18) should be the same and equal to the sediment concentration at the open boundary (the outside area). This constant is called the global equilibrium concentration c_E, with $C_f = C_c = C_d = c_o = c_E$.

Any deviation from this rule implies a redefinition of the morphological equilibrium state.

References

Carrasco, A.R., Ferreira, Ó., Roelvink, D., 2016. Coastal lagoons and rising sea level: A review. Earth Sci. Rev. 154, 356−368. https://doi.org/10.1016/j.earscirev.2015.11.007.

Cowell, P.J., Stive, M.J.E., Niedoroda, A., de Vriend, H.J., Swift, D., Kaminsky, G.M., Capobianco, M., 2003. The coastal-tract (part 1): A conceptual approach to aggregated modelling of low-order coastal change. J. Coast. Res. 19(4), 812−827.

Dam, G., van der Wegen, M., Labeur, R.J., Roelvink, D., 2016. Modeling centuries of estuarine morphodynamics in the Western Scheldt Estuary. Geophys. Res. Lett. 43(8), 3839−3847. https://doi.org/10.1002/2015gl066725.

Deltacommissie, 2008. Working Together with Water, Report of Deltacommissie. Deltacommissie, Rotterdam.

Di Silvio, G., 1989. Modelling the morphological evolution of tidal lagoons and their equilibrium configurations. In: Proceedings of the 13th Congress of IAHR. IAHR, pp. C-169−C-175.

Di Silvio, G., Dall'Angelo, C., Bonaldo, D., Fasolato, G., 2010. Long-term model of planimetric and bathymetric evolution of a tidal lagoon. Cont. Shelf Res. 30(8), 894−903. https://doi.org/10.1016/j.csr.2009.09.010.

Elias, E.P.L., van der Spek, A.J.F., Wang, Z.B., de Ronde, J.G., 2012. Morphodynamic development and sediment budget of the Dutch Wadden Sea over the last century. Neth. J. Geosci. 91(3), 293−310. https://doi.org/10.1017/s0016774600000457.

Eysink, W.D., 1990. Morphological response of tidal basins to change. In: Proceedings of the 22nd International Conference on Coastal Engineering. ASCE, Delft, pp. 1948−1961. https://doi.org/10.1061/9780872627765.149.

Eysink, W.D., Biegel, E.J., 1992. Impact of Sea Level Rise on the Morphology of the Wadden Sea in the Scope of its Ecological Function. ISOS*2 Project, Phase 2, Report H1300. WL|Delft Hydraulics, Delft.

Fokker, P.A., van Leijen, F., Orlic, B., van der Marel, H., Hanssen, R., 2018. Subsidence in the Dutch Wadden Sea. Neth. J. Geosci. 97(3), 129−181. https://doi.org/10.1017/njg.2018.9.

Galappatti, G., Vreugdenhil, C.B., 1985. A depth integrated model for suspended sediment transport. J. Hydraul. Res. 23(4), 359−375. https://doi.org/10.1080/00221688509499345.

Hinkel, J., Nicholls, R.J., Tol, R.S.J., Wang, Z.B., Hamilton, J.M., Boot, G., Vafeidis, A.T., McFadden, L., Ganopolski, A., Klein, R.J.T., 2013. A global analysis of erosion of sandy beaches and sea-level rise: An application of DIVA. Global Planet. Change 111, 150−158. https://doi.org/10.1016/j.gloplacha.2013.09.002.

Jeuken, M.C.J.L., Wang, Z.B., Keiller, D., Townend, I.H., Like, G.A., 2003. Morphological response of estuaries to nodal tide variation. In: Proceedings of International Conference on Estuaries and Coasts (ICEC-2003), pp. 166−173.

Koninklijk Nederlands Meteorologisch Instituut (KNMI), 2017. Extreme Zeespiegelstijging in de 21e Eeuw. KNMI (in Dutch).

Kragtwijk, N.G., Zitman, T.J., Stive, M.J.F., Wang, Z.B., 2004. Morphological response of tidal basins to human interventions. Coastal Eng. 51(3), 207−221. https://doi.org/10.1016/j.coastaleng.2003.12.008.

Lacey, G., 1930. Stable channels in alluvium. In: Minutes of the Proceedings of the Institution of Civil Engineers, vol. 229, pp. 259−292. https://doi.org/10.1680/imotp.1930.15592.

Langbein, W.B., 1963. The hydraulic geometry of a shallow estuary. Bull. Int. Assoc. Sci. Hydrol. 8(3), 84−94. https://doi.org/10.1080/02626666309493340.

Le Bars, D., Drijfhout, S., de Vries, H., 2017. A high-end sea level rise probabilistic projection including rapid Antarctic ice sheet mass loss. Environ. Res. Lett. 12(4), 44013. https://doi.org/10.1088/1748-9326/aa6512.

Leopold, L.B., Langbein, W.B., 1962. The Concept of Entropy in Landscape Evolution. Geological Survey Professional Paper 500-A. United States Government Printing Office, Washington, D.C. https://doi.org/10.3133/pp500a.

Lodder, Q.J., Wang, Z.B., Elias, E.P.L., van der Spek, A.J.F., de Looff, H., Townend, I.H., 2019. Future response of the Wadden Sea tidal basins to relative sea-level rise: An aggregated modelling approach. Water 11(10). https://doi.org/10.3390/w11102198.

Meehl, G., Stocker, T.F., Collins, W.D., Friedlingstein, P., Gaye, A.T., Gregory, J.M., Kitoh, A., Knutti, R., Murphy, J.M., Noda, A., et al., 2007. Global climate projections, 2007. In: Solomon, S., Qin, D., Manning, M., Chen, Z., Marquis, M., Averyt, K.B., Tignor, M., Mille, H.L., eds., Climate Change 2007: The Physical Science Basis. Contribution of Working Group 1 to the Fourth Assessment Report of the Intergovernmental Panel on Climate Change. Cambridge University Press, Cambridge, p. 996.

Nichols, M.M., 1989. Sediment accumulation rates and relative sea-level rise in lagoons. Mar. Geol. 88(3−4), 201−219. https://doi.org/10.1016/0025-3227(89)90098-4.

O'Connor, B.A., Nicholson, J., Rayner, R., 1990. Estuary geometry as a function of tidal range. In: Proceedings of the 22nd International Conference on Coastal Engineering. ASCE, pp. 3050−3062. https://doi.org/10.1061/9780872627765.233.

Renger, E., Partenscky, H.W., 1974. Stability criteria for tidal basins. In: Proceedings of the 14th Coastal Engineering Conference, vol. 2. ASCE, pp. 1605−1618.

Roelvink, D., Reniers, A., 2012. A guide to modelling coastal morphology. In: Advances in Coastal and Ocean Engineering, vol. 12. World Scientific Publishing, Singapore. https://doi.org/10.1142/7712.

Rossington, K., Nicholls, R.J., Knaapen, M.A.F., Wang, Z.B., 2007. Morphological behaviour of UK estuaries under conditions of accelerating sea level rise. In: Dohmen-Janssen, C.M., Hulscher, S.J.M.H., eds., River, Coastal and Estuarine Morphodynamics: RCEM2007. Taylor & Francis. https://doi.org/10.1201/noe0415453639-c16.

Soulsby, R., 1997. Dynamics of Marine Sands. Thomas Telford, London.

Spearman, J., 2007. Hybrid Modelling of Managed Realignment, Series No. TR157. HR Wallingford, Wallingford.

Stive, M.J.F., Roelvink, J.A., de Vriend, H.J., 1990. Large-scale coastal evolution concept. The Dutch Coast, Paper No. 9. In: Louisse, C.J., Stive, M.J.F., Wiersma, J., eds., Proceedings of the 22nd International Conference on Coastal Engineering, 1990: The Dutch Coast. ASCE, p. 13. https://doi.org/10.1061/9780872627765.150.

Stive, M.J.F., Capobianco, M., Wang, Z.B., Ruol, P., Buijsman, M.C., 1998. Morphodynamics of a tidal lagoon and adjacent coast. In: Dronkers, J., Scheffers, M.B.A.M., eds., Proceedings of the 8th International Biennial Conference on Physics of Estuaries and Coastal Seas. A.A. Balkema, pp. 397−407.

Stive, M.J.F., Wang, Z.B., 2003. Morphodynamic modelling of tidal basins and coastal inlets. In: Lakkhan, C., ed., Advances in Coastal Modelling. Elsevier Sciences, Amsterdam, pp. 367−392. https://doi.org/10.1016/s0422-9894(03)80130-7.

Townend, I.H., Wang, Z.B., Rees, J.G., 2007. Millennial to annual volume changes in the Humber Estuary. Proc. R. Soc. A Math. Phys. Eng. Sci. 463(2079), 837−854. https://doi.org/10.1098/rspa.2006.1798.

Townend, I.H., 2010. An exploration of equilibrium in Venice Lagoon using an idealised form model. Cont. Shelf Res. 30(8), 984−999. https://doi.org/10.1016/j.csr.2009.10.012.

Townend, I.H., Wang, Z.B., Stive, M.J.E., Zhou, Z., 2016a. Development and extension of an aggregated scale model, part 1: Background to ASMITA. China Ocean Eng. 30(4), 482−504. https://doi.org/10.1007/s13344-016-0030-x.

Townend, I.H., Wang, Z.B., Stive, M.J.E., Zhou, Z., 2016b. Development and extension of an aggregated scale model, part 2: Extensions to ASMITA. China Ocean Eng. 30(5), 651−670. https://doi.org/10.1007/s13344-016-0042-6.

van der Spek, A.J.F., Beets, D.J., 1992. Mid-Holocene evolution of a tidal basin in the western Netherlands: A model for future changes in the northern Netherlands under conditions of accelerated sea-level rise?

Sediment. Geol. 80(3−4), 185−197. https://doi.org/10.1016/0037-0738(92)90040-x.

van der Wegen, M., Wang, Z.B., Townend, I.H., Savenije, H.H.G., Roelvink, J.A., 2009. Long-term, morphodynamic modeling of equilibrium in an alluvial tidal basin using a process-based approach. In: Proceedings of the 6th Symposium on River, Coastal and Estuarine Morphodynamics. IAHR.

van Goor, M.A., Zitman, T.J., Wang, Z.B., Stive, M.J.F., 2003. Impact of sea-level rise on the morphological equilibrium state of tidal inlets. Mar. Geol. 202, 211−227. https://doi.org/10.1016/s0025-3227(03)00262-7.

van Rijn, L.C., 1993. Principles of Sediment Transport in Rivers, Estuaries and Coastal Seas. Aqua Publications, Amsterdam.

Vermeersen, L.L.A., Slangen, A.B.A., Gerkema, T., Baart, F., Cohen, K.M., Dangendorf, S., Duran-Matute, M., Frederikse, T., Grinsted, A., Hijma, M.P., et al., 2018. Sea level change in the Dutch Wadden Sea. Neth. J. Geosci. 97(3), 79−127. https://doi.org/10.1017/njg.2018.7.

Walton, T.L., Adams, W.D., 1976. Capacity of inlet outer bars to store sand. In: Proceedings of the 15th Coastal Engineering Conference. ASCE, Honolulu, pp. 1919−1937.

Wang, Z.B., 1992. Theoretical analysis on depth-integrated modelling of suspended Sediment transport. J. Hydraul. Res. 30(3), 403−420. https://doi.org/10.1080/00221689209498927.

Wang, Z.B., Karssen, B., Fokkink, R.J., Langerak, A., 1998. A dynamic-empirical model for estuarine morphology. In: Dronkers, J., Scheffers, M.B.A.M., eds., Physics of Estuaries and Coastal Seas. A.A. Balkema, Rotterdam, pp. 279−286.

Wang, Z.B., de Vriend, H.J., Stive, M.J.F., Townend, I.H., 2008. On the parameter setting of semi-empirical long-term morphological models for estuaries and tidal lagoons. In: Dohmen-Janssen, C.M., Hulscher, S.J.M.H., eds. River, Coastal and Estuarine Morphodynamics: RCEM 2007. Taylor & Francis, pp. 103−111. https://doi.org/10.1201/noe0415453639-c14.

Wang, Z.B., Hoekstra, P., Burchard, H., Ridderinkhof, H., de Swart, H.E., Stive, M.J.F., 2012. Morphodynamics of the Wadden Sea and its barrier island system. Ocean Coast. Manag. 68, 39−57. https://doi.org/10.1016/j.ocecoaman.2011.12.022.

Wang, Z.B., Townend, I.H., 2012. Influence of the nodal tide on the morphological response of estuaries. Mar. Geol. 291−294, 73−82. https://doi.org/10.1016/j.margeo.2011.11.007.

Wang, Z.B., Elias, E.P.L., van der Spek, A.J.F., Lodder, Q.L., 2018. Sediment budget and morphological development of the Dutch Wadden Sea: Impact of accelerated sea-level rise and subsidence until 2100. Neth. J. Geosci. 97(3), 183−214. https://doi.org/10.1017/njg.2018.8.

Winterwerp, J.C., van Kesteren, W.G.M., van Prooijen, B., Jacobs, W., 2012. A conceptual framework for shear flow-induced erosion of soft cohesive sediment beds. J. Geophys. Res. 117(C10). https://doi.org/10.1029/2012jc008072.

Wright, A.D., Townend, I.H., 2006. Predicting long term estuary evolution using regime theory. In: Littoral 2006 Conference Proceedings. Gdańsk University of Technology, Gdańsk, pp. 1−9.